Electronic Supplementary Information

Brønsted Acid-Base Ionic Liquids for Fuel Cell Electrolytes

Hirofumi Nakamoto and Masayoshi Watanabe*

Department of Chemistry and Biotechnology, Yokohama National University

79-5 Tokiwadai, Hodogaya-ku, Yokohama 240-8501, Japan

E-mail: mwatanab@ynu.ac.jp; Fax: +81-45-339-3955; Tel: +81-45-339-3955

Experimental Details

Materials. All of the amines and acids in this study were reagent grade and were used as received. Appropriate amounts of each aliphatic amine and each acid, strictly maintained at the equimolar ratio, were weighed in an argon atmosphere glove box (VAC, $[O_2] < 1$ ppm, $[H_2O] < 1$ ppm) and mixed under argon atmosphere with cooling. In particular, when super-strong acids such as $HN(T_f)_2$ and T_fOH were used, vigorous cooling was necessary because of the extremely exothermic reactions. The mixtures were then evacuated for 12 h at 150 °C for the protic salts based on $HN(T_f)_2$, T_fOH, and H_2SO_4, at 130 °C for those based on CH_3SO_3H, and at 100 °C for those based on H_3PO_4 and H_2PHO_3, in order to eliminate excess amine or acid, if any. At these temperatures, all of the salts became homogenous liquids (protic ILs). All of the protic ILs were stored and handled in the glove box. The stoichiometry of the protic ILs could be checked by the following thermal analysis (DSC and TG).

Thermal Properties. DSC was carried out with a Seiko Instruments Model 220C differential scanning calorimeter under N_2 atmosphere. The samples for the DSC measurements were tightly sealed in Al pans in the glove box. The DCS samples were first heated up to temperatures higher than the T_ms of each protic IL, cooled down to -150 °C , and then heated again to 150 °C at 10 °C min^{-1} in order to eliminate the thermal histories. The thermograms during the reheating scans were used for the determination of the thermal transitions. The T_ms were defined as the onset temperatures of the endothermic peaks, and the T_gs were defined as mid-temperatures of the heat capacity changes. The T_ds were measured on a Seiko Instruments thermogravimetry/differential thermoanalyzer Model 6200 from 30 °C to 550 °C at a heating rate of 10 °C min^{-1} under N_2 atmosphere with open Al pans. The T_ds were defined as the onset temperatures of the weight loss.

Self-Diffusion Coefficients. The diffusion measurements were conducted by use of a Techmag Appolo system with a 4.7 T wide-bore superconducting magnet equipped with a JEOL pulse field gradient probe and a current amplifier. The square-gradient-pulse, providing gradient strength up to 10 Tm^{-1}, was used throughout the measurements. The ^{1}H self-diffusion coefficients were measured using a modified stimulated echo pulse sequence, (i.e., $90° - \tau_1 - 90° - \tau_2 - 90° - \tau_1 -$ acquisition), and ^{19}F self-diffusion coefficients were measured with a modified Hahn spin echo sequence, (i.e., $90° - \tau - 180° - \tau -$ acquisition), incorporating a gradient pulse in each τ_1 or τ period. The free diffusion echo signal attenuation, E, is related to the experimental parameters by

$$\ln E = \ln(S/S_{g=0}) = -\gamma^2 g^2 D \delta^2 (\Delta - \delta/3)$$

where S is the spin-echo signal intensity, δ is the duration of the field gradient with magnitude g, γ is the gyromagnetic ratio, D is the self-diffusion coefficient, and Δ is the interval between two gradient pulses and was mainly held at 30 ms in this study. A recycle delay sufficient to allow full relaxation (i.e., $>3T_1$) was used between each transition. The measurements were checked for convection effects by changing Δ. The measurements for the cationic and anionic self-diffusion coefficients were made by use of the ^{1}H (270.2 MHz) and ^{19}F (254.2 MHz) nuclei, respectively. The measurements were performed in the temperature range from 30 to 130 °C with the samples thermally equilibrated at the initial temperature for 0.5 h prior to the measurements. The samples were inserted into a 5-mm (o.d.) NMR microtube (BMS-005J, Shigemi) in the glove box to a height of 5 mm.

Ionic Conductivities. The ionic conductivities were determined by the complex impedance method with a Hewlett-Packard 4192A LF impedance analyzer in the frequency range from 5 Hz to 13 MHz. The samples were filled in a dip-type glass cell with two Pt wires fixed at a constant electrode distance in the glove box and were thermally equilibrated at each temperature for at least 1 h (Yashima, BX-10) prior to the measurements. The cell constant was determined by use of a 0.1 M KCl standard solution (Kanto) at 30 °C.

Electrochemical Polarization. Cyclic voltammetry was measured at 150 °C for the protic ILs such as [dema]/[T_fOH] = 1/1 with a two-compartment glass cell sparged with dry N_2, H_2, or O_2 gases. The counter electrode (CE) was a platinized Pt wire, and the working electrode (WE) was a Pt wire (0.5 mm diameter, 5 mm length). The reference electrode (RE) was a Pt wire in a H_2-sparged solution, placed close to the WE through a Luggin capillary, as a reversible hydrogen electrode (RHE) for all of the experiments in this study. The surface area of the WE was estimated from the hydrogen desorption peak of the cyclic voltammetry measured in a 1 M H_2SO_4 aqueous solution at 30 °C. For the fuel cell polarization experiments, either the protic IL or a typical H^+-conducting electrolyte was placed in a U-shaped glass tube; from each end, a Pt-wire electrode

(0.5-mm diameter, 5-mm length) was inserted, where the distance between the two electrodes was 2.5 cm; O_2 or H_2 gases were sparged around each Pt electrode though fine Teflon tubes at a flow rate of 2 $mLmin^{-1}$. The current density of the cells was calculated based on the surface area of the cathode (O_2 electrode), which was also determined from the hydrogen desorption peak, as mentioned above. The electrochemical control was accomplished with use of a Solartron electrochemical interface (Model 1287). The temperature was regulated by use of a constant temperature chamber (Yamato DKN 611).

Thermal Properties and Ionic Conductivities of Protic ILs

The thermal properties and ionic conductivities for all of the protic ILs investigated in this study are summarized in ***Tables SI-1~SI-6***. It can be seen from these data that [dema]/[T_fOH] = 1/1 has the most favorable properties of the protic ILs in this study in terms of the thermal stability, the liquid temperature range, and the ionic conductivity.

Electroactivity of Typical Protic ILs

CVs for typical protic ILs are shown in ***Figures SI-1~SI-4***. The open circuit potential (OCP) values of O_2 reduction for the protic ILs investigated in this study are summarized in ***Tables SI-1~ SI-6***. In the case of [dema]/[HN(T_f)$_2$] = 1/1 (***Figure SI-1***), the structural change of acid from T_fOH (***Figure 1a***) to HN(T_f)$_2$ greatly affects the O_2 reduction and H_2 oxidation, even though the base was identical in [dema]/[HN(T_f)$_2$] = 1/1 and [dema]/[T_fOH] = 1/1. The O_2 reduction and H_2 oxidation reactions became quite slow, compared with those of [dema]/[T_fOH] = 1/1. This indicates that the facile O_2 reduction and H_2 oxidation, seen in [dema]/[T_fOH] = 1/1, is not caused by the use of dema.

When strong oxoacids such as H_2SO_4 (***Figure SI-2, Table SI-2***) and CH_3SO_3H (***Figure SI-3, Table SI-3***) are used in the protic ILs, their O_2 reduction starts from close to 1 V; however, the O_2 reduction and H_2 oxidation reactions were more sluggish and the electrochemical stability was poorer than those of [dema]/[T_fOH] = 1/1. The protic ILs from strong or super-strong oxoacids appear to give better oxygen reduction kinetics, compared with those from HN(T_f)$_2$. Although comparable electrochemical activity to [dema]/[T_fOH] = 1/1 can be found in [dmea]/[T_fOH] = 1/1 (***Figure SI-4***), its liquid temperature range and ionic conductivity (***Table SI-1***) are inferior to those of [dema]/[T_fOH] = 1/1.

It is clear from these results that [dema]/[T_fOH] = 1/1 has the most favorable properties of the protic ILs in this study in terms of the thermal stability, the liquid temperature range, the ionic conductivity, and the electrochemical activity of H_2 and O_2.

Table SI-1 Thermal properties, ionic conductivities and open circuit potential (OCP) of O_2 reduction for protic ionic liquids based on $\mathrm{T_fOH}$

ionic liquid [Base]/[Acid] = 1/1	T_g[a] / °C	T_m[b] / °C	T_d[c] / °C	σ[d] at 120 °C / 10^{-2} S cm^{-1}	OCP of O_2 reduction / V vs. RHE at 150 °C
[ea]/[$\mathrm{T_fOH}$]	——	179	372	——[e]	——[e]
[ba]/[$\mathrm{T_fOH}$]	——	178	348	——[e]	——[e]
[ha]/[$\mathrm{T_fOH}$]	——	169	358	——[e]	——[e]
[dea]/[$\mathrm{T_fOH}$]	——	125	362	——[e]	——[e]
[dba]/[$\mathrm{T_fOH}$]	——	143	351	——[e]	——[e]
[dha]/[$\mathrm{T_fOH}$]	——	120	356	——[e]	——[e]
[Pp]/[$\mathrm{T_fOH}$]	——	142	383	——[e]	——[e]
[tma]/[$\mathrm{T_fOH}$]	——	146	355	——[e]	——[e]
[tea]/[$\mathrm{T_fOH}$]	——	34.3	358	2.76	0.94
[tba]/[$\mathrm{T_fOH}$]	——	128	353	——[e]	——[e]
[tha]/[$\mathrm{T_fOH}$]	-83	-1.0	361	0.209	——[e]
[dmea]/[$\mathrm{T_fOH}$]	-117	41.6	360	5.6	1.01
[dema]/[$\mathrm{T_fOH}$]	——	-13.1	360	4.33	1.03
[EPp]/[$\mathrm{T_fOH}$]	-76.2	52	372	2.58	1.08
[tbma]/[$\mathrm{T_fO}$]	——	87.2	350	0.614	——[e]

[a] Glass transition temperature. [b] Melting point. [c] Onset temperature of decreasing weight. [d] Ionic conductivity. [e] Not measured.

ea : ethylamine, ba : butylamine, ha : hexylamine, dea : diethylamine, dba : dibutylamine, dha : dihexylamine, Pp : piperidine, tma : trimethylamine, tea : triethylamine, tba : tributylamine, tha : trihexylamine, dmea : dimethylethylamine, dema : diethylmethylamine, EPp : N-ethylpiperidine, tbma : tributylmethyl ammonium, $\mathrm{T_fOH}$: trifluoromethanesulfonic acid

Table SI-2 Thermal properties, ionic conductivities and open circuit potential (OCP) of O_2 reduction for protic ionic liquids based on H_2SO_4

ionic liquid [Base]/[Acid] = 1/1	T_g[a] / °C	T_m[b] / °C	T_d[c] / °C	σ[d] at 120 °C / 10^{-2} S cm^{-1}	OCP of O_2 reduction / V vs. RHE at 150 °C
[ea]/[H_2SO_4]	-64.1	39.7	262	3.41	—[e]
[ba]/[H_2SO_4]	-50.1	—	282	0.0665	0.45
[ha]/[H_2SO_4]	-57	26.4	269	—[e]	—[e]
[dea]/[H_2SO_4]	-67.1	60.5	262	1.97	0.63
[dba]/[H_2SO_4]	-62.8	54.8	260	0.372	—[e]
[dha]/[H_2SO_4]	—	134	269	—[e]	—[e]
[Pp]/[H_2SO_4]	-48.8	66.8	273	0.791	—[e]
[tea]/[H_2SO_4]	—	74.7	270	1.31	0.55
[tba]/[H_2SO_4]	-56	73	254	0.0922	—[e]
[tha]/[H_2SO_4]	-62.1	28.8	247	0.0236	—[e]
[dmea]/[H_2SO_4]	-75.9	—	271	3.83	—[e]
[dema]/[H_2SO_4]	-82.1	—	268	1.97	0.60
[EPp]/[H_2SO_4]	-53.7	—	246	0.88	0.79
[tbma]/[HSO_4]	-26.5	96.5	280	0.141	0.79

[a] Glass transition temperature. [b] Melting point. [c] Onset temperature of decreasing weight. [d] Ionic conductivity. [e] Not measured.

ea : ethylamine, ba : butylamine, ha : hexylamine, dea : diethylamine, dba : dibutylamine, dha : dihexylamine, Pp : piperidine, tea : triethylamine, tba : tributylamine, tha : trihexylamine, dmea : dimethylethylamine, dema : diethylmethylamine, EPp : N-ethylpiperidine, tbma : tributylmethyl ammonium

Table SI-3 Thermal properties, ionic conductivities and open circuit potential (OCP) of O_2 reduction for protic ionic liquids based on CH_3SO_3H

ionic liquid [Base]/[Acid] = 1/1	T_g[a] / °C	T_m[b] / °C	T_d[c] / °C	σ[d] at 120 °C / 10^{-2} S cm^{-1}	OCP of O_2 reduction / V vs. RHE at 150 °C
[ea]/[CH_3SO_3H]	——	137	230	—[e]	—[e]
[ba]/[CH_3SO_3H]	——	117	249	—[e]	—[e]
[ha]/[CH_3SO_3H]	——	169	353	—[e]	—[e]
[dea]/[CH_3SO_3H]	-67.8	31.4	185	—[e]	0.81
[dba]/[CH_3SO_3H]	-60.6	41.1	249	0.829	—[e]
[dha]/[CH_3SO_3H]	——	52.2	284	0.317	—[e]
[Pp]/[CH_3SO_3H]	——	111	247	1.60	—[e]
[tea]/[CH_3SO_3H]	-62.1	17.4	225	1.63	0.80
[tba]/[CH_3SO_3H]	-69.4	41	254	0.752	—[e]
[tha]/[CH_3SO_3H]	——	——	266	—[e]	—[e]
[dema]/[CH_3SO_3H]	-72.2	10.6	180	2.22	—[e]
[EPp]/[CH_3SO_3H]	-73.3	67.6	201	1.27	—[e]
[tbma]/[CH_3SO_3]	-17.3	78	268	0.372	—[e]

[a] Glass transition temperature. [b] Melting point. [c] Onset temperature of decreasing weight. [d] Ionic conductivity. [e] Not measured.

ea : ethylamine, ba : butylamine, ha : hexylamine, dea : diethylamine, dba : dibutylamine, dha : dihexylamine, Pp : piperidine, tea : triethylamine, tba : tributylamine, tha : trihexylamine, dema : diethylmethylamine, EPp : N-ethylpiperidine, tbma : tributylmethyl ammonium

Table SI-4 Thermal properties and ionic conductivities for protic ionic liquids based on H_2PHO_3

ionic liquid [Base]/[Acid] = 1/1	T_g[a] / °C	T_m[b] / °C	T_d[c] / °C	σ[d] at 120 °C / 10^{-2} S cm^{-1}
[ba]/[H_2PHO_3]	——	83.5	157	——[e]
[ha]/[H_2PHO_3]	-67.6	78.7	160	0.252
[dea]/[H_2PHO_3]	——	——	161	——[e]
[dba]/[H_2PHO_3]	——	69.2	170	0.186
[dha]/[H_2PHO_3]	——	145	181	——[e]
[Pp]/[H_2PHO_3]	-45.2	82.9	156	0.278
[tea]/[H_2PHO_3]	-78.4	——	135	——[e]
[tba]/[H_3PO_3]	-60	——	150	0.126
[tha]/[H_2PHO_3]	-59.8	——	158	——[e]
[dema]/[H_2PHO_3]	-84.6	——	137	——[e]
[EPp]/[H_2PHO_3]	-71.3	——	136	——[e]
[tbma]/[$HPHO_3$]	-13.4	82.5	198	0.0634

[a] Glass transition temperature. [b] Melting point. [c] Onset temperature of decreasing weight. [d] Ionic conductivity. [e] Not measured.

ba : butylamine, ha : hexylamine, dea : diethylamine, dba : dibutylamine, dha : dihexylamine, Pp : piperidine, tea : triethylamine, tba : tributylamine, tha : trihexylamine, dema : diethylmethylamine, EPp : N-ethylpiperidine, tbma : tributylmethyl ammonium

Table SI-5 Thermal properties and ionic conductivities for protic ionic liquids based on H_3PO_4

ionic liquid [Base]/[Acid] = 1/1	T_g[a] / °C	T_m[b] / °C	T_d[c] / °C	σ[d] at 120 °C / 10^{-2} S cm^{-1}
[ba]/[H_3PO_4]	—	120	170	—[e]
[ha]/[H_3PO_4]	—	125	195	—[e]
[dea]/[H_3PO_4]	—	—	140	—[e]
[dba]/[H_3PO_4]	—	120	166	—[e]
[dha]/[H_3PO_4]	—	133	179	—[e]
[Pp]/[H_3PO_4]	—	—	188	—[e]
[tea]/[H_3PO_4]	-27.8	—	175	—[e]
[tba]/[H_3PO_4]	-6.5	—	150	—[e]
[tha]/[H_3PO_4]	-24.3	—	167	—[e]
[dema]/[H_3PO_4]	-37.9	—	175	0.651
[EPp]/[H_3PO_4]	-11.7	—	144	—[e]
[tbma]/[H_2PO_4]	—	141	196	—[e]

[a] Glass transition temperature. [b] Melting point. [c] Onset temperature of decreasing weight. [d] Ionic conductivity. [e] Not measured.

ba : butylamine, ha : hexylamine, dea : diethylamine, dba : dibutylamine, dha : dihexylamine, Pp : piperidine, tea : triethylamine, tba : tributylamine, tha : trihexylamine, dema : diethylmethylamine, EPp : N-ethylpiperidine, tbma : tributylmethyl ammonium

Table SI-6 Thermal properties, ionic conductivities and open circuit potential (OCP) of O_2 reduction for protic ionic liquids based on $HN(T_f)_2$

ionic liquid [Base]/[Acid] = 1/1	T_g[a] / °C	T_m[b] / °C	T_d[c] / °C	σ[d] at 120 °C / 10^{-2} S cm^{-1}	OCP of O_2 reduction / V vs. RHE at 150 °C
[dmea]/[$HN(T_f)_2$]	-42.4	65.6	377	4.62	—[e]
[dema]/[$HN(T_f)_2$]	-67.3	24	375	4.05	0.77
[Im]/[$HN(T_f)_2$]	—[f]	73[f]	379[f]	2.40[f]	0.57
[BIm]/[$HN(T_f)_2$][f]	—	117	390	1.00	0.87

[a] Glass transition temperature. [b] Melting point. [c] Onset temperature of decreasing weight. [d] Ionic conductivity. [e] Not measured. [f] The datas for [Im]/[$HN(T_f)_2$] = 1/1 and [BIm]/[$HN(T_f)_2$] = 1/1 are cited from ref. 15 and 16, respectively.

dmea : dimethylethylamine, dema : diethylmethylamine, Im : imidazole, BIm: benzimidazole, $HN(T_f)_2$: bis(trifuluoromethane sulfonyl) imide

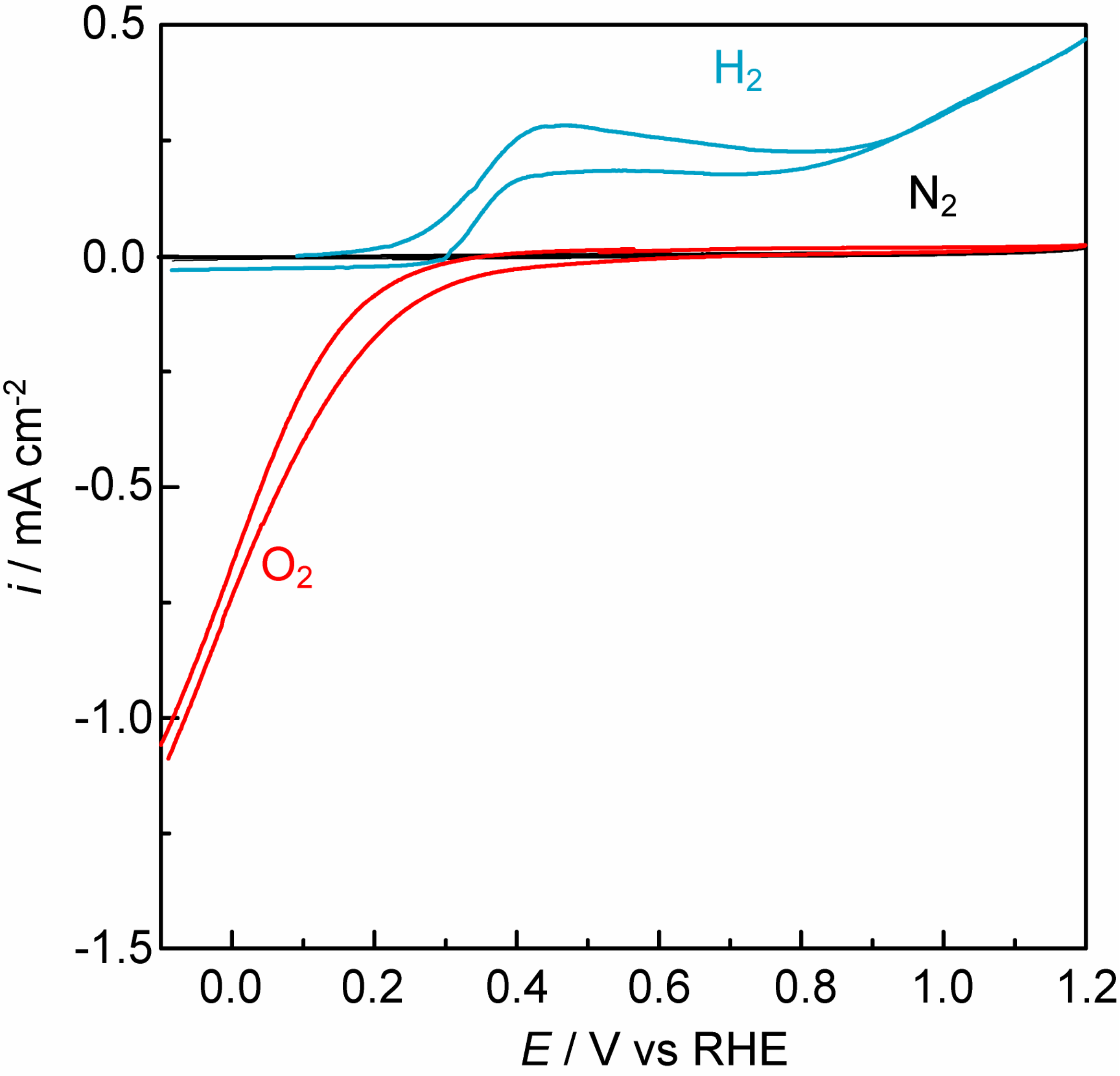

Fig. SI-1. Cyclic voltammograms (10 mV s^{-1}) for [dema]/[$HN(T_f)_2$] = 1/1 at 150 °C.

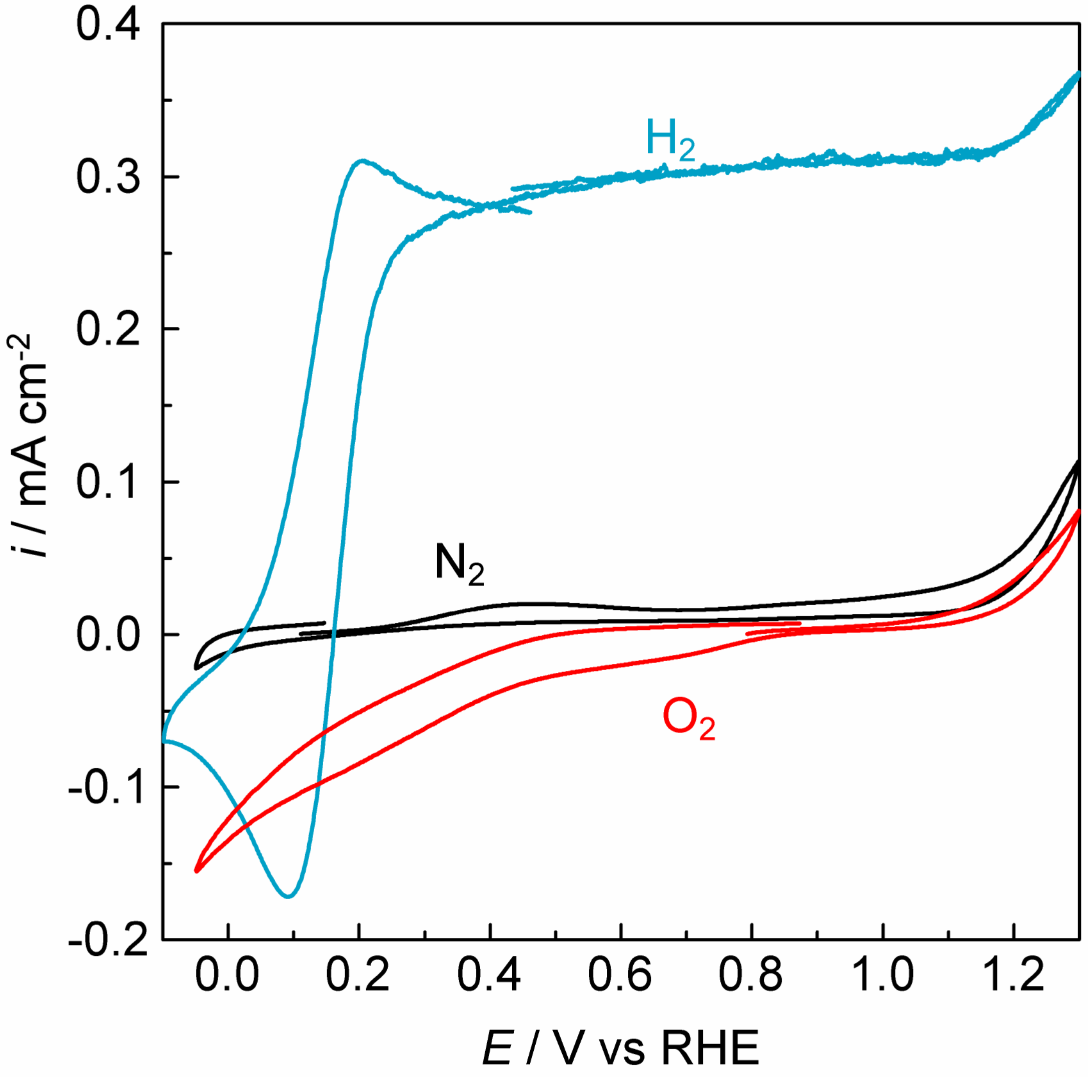

Fig. SI-2. Cyclic voltammograms (10 mV s^{-1}) for [tbma]/[HSO_4] = 1/1 at 150 °C.

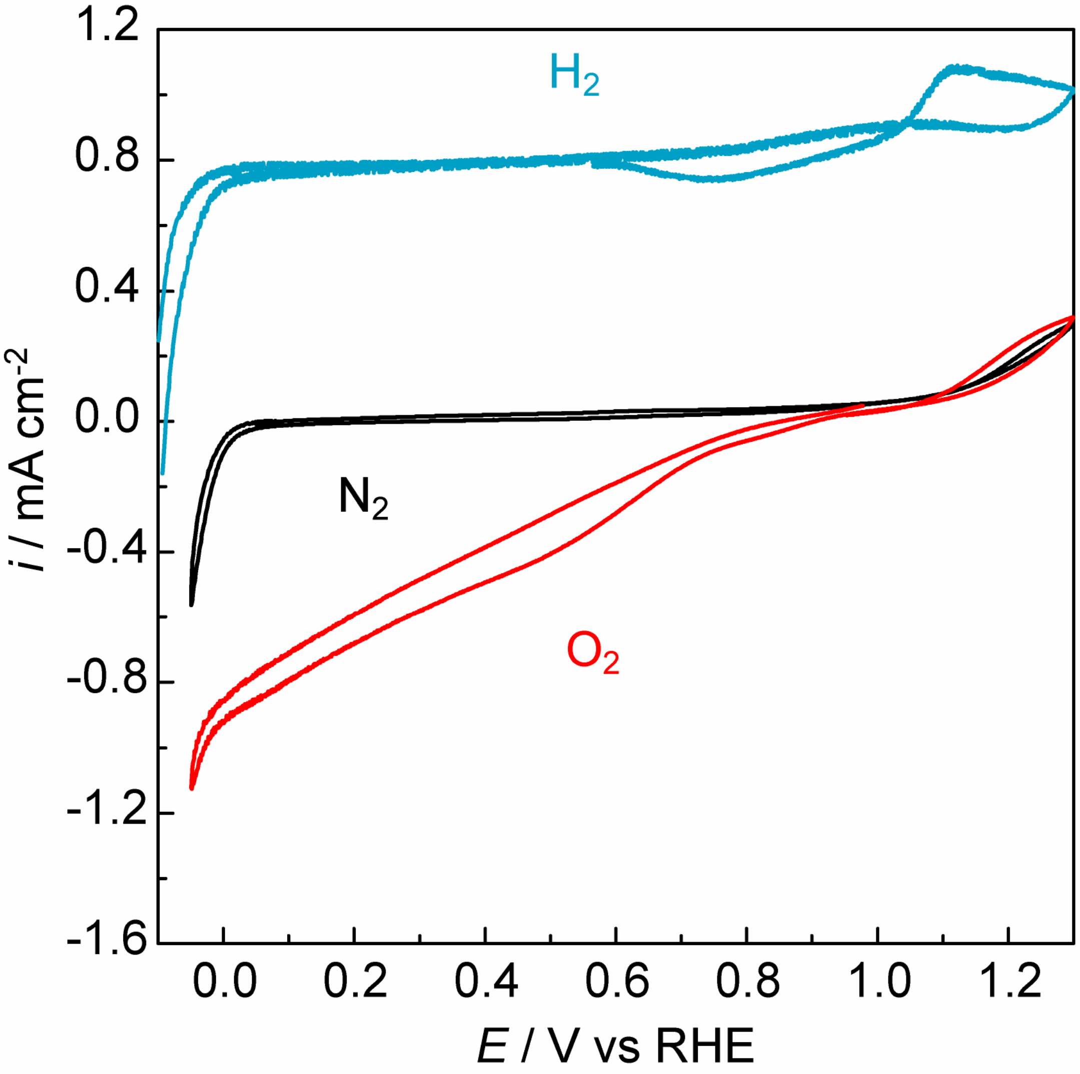

Fig. SI-3. Cyclic voltammograms (10 mV s^{-1}) for [dea]/[CH_3SO_3H] = 1/1 at 150 ^{o}C.

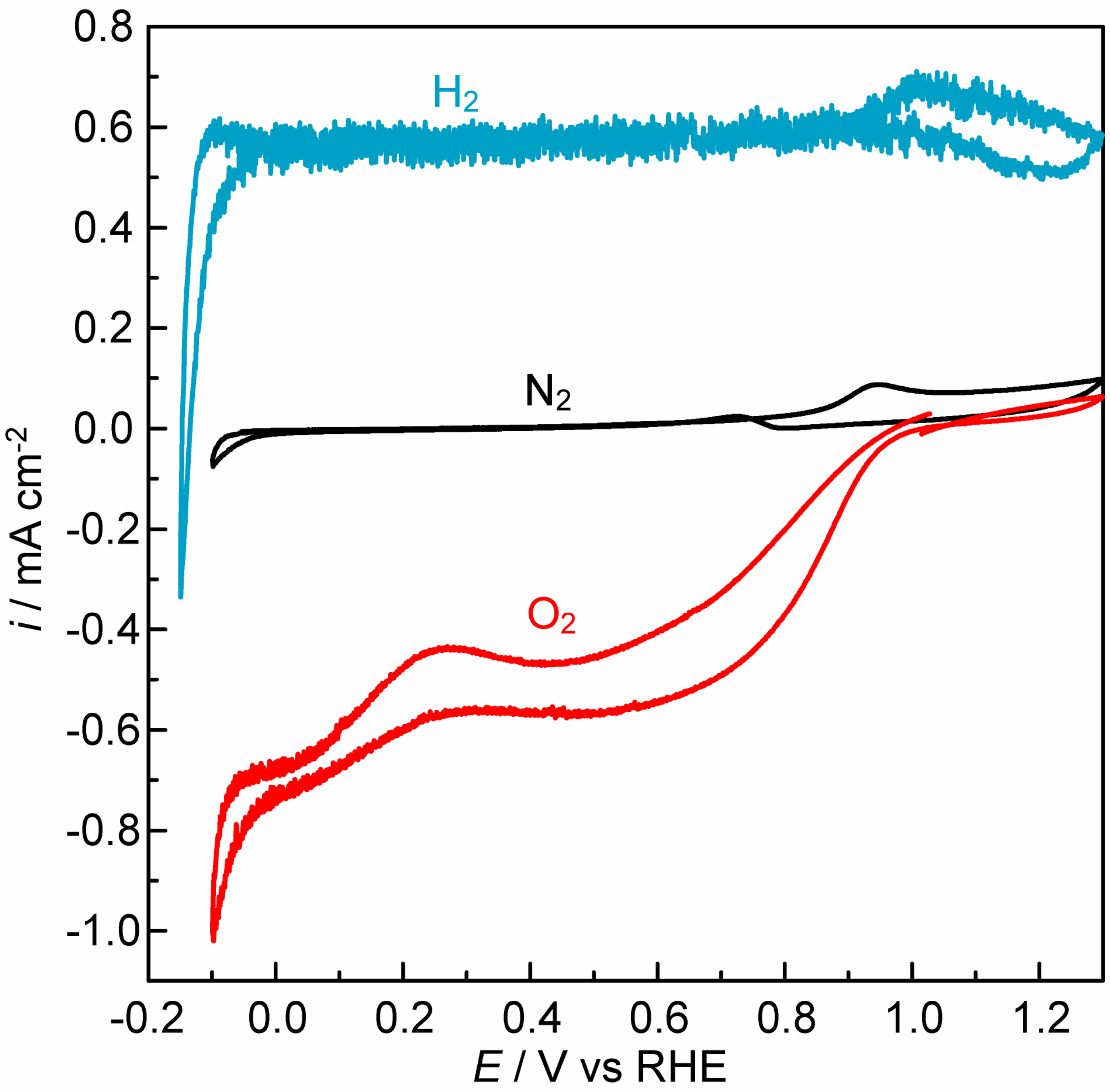

Fig. SI-4. Cyclic voltammograms (10 mV s^{-1}) for [dmea]/[T_fOH] = 1/1 at 150 °C.